

REFERENCES

Chapter-1

1. Yoshida S. et. al., *Astroparticle physics*, 3(1995)105.
2. Bezrukov L.B., Bugaev E.V., *Proc. of the 17th ICRC*, Paris, 7(1981)50.
3. Wdowczyk J., *Proc. of the 8th ICRC*, London, 2(1965)691.
4. Nishimura J. and Kamata K., *Prog. Theor. Phys.*, 5(1950)899, 6 (1951) 628.
5. Greisen K., *Annu. Rev. Nucl. Sci.*, 10(1960)63.
6. Hillas A.M. and Lapikens J., *Proc. of the 15th ICRC*, Plovdiv, 8 (1977)460.
7. Linsley J., *Proc. of the 15th ICRC*, Plovdiv, 12(1977) 56.
8. Capdevielle J.N., Procureur R. and Gawin J., *Proc. of the 18th ICRC*, Bangalore, 11 (1983)307.
9. Capdevielle J.N. and Gawin J., *Proc. of the 18th ICRC*, Bangalore, 11(1983) 303.
10. Galbraith W., *Extensive Air Shower*, 1958, 111.
11. Trzuppek A., Lu Y. and Poirier J., *Proc. of the 23rd ICRC*, Calgary, 4(1993) 359.
12. Yash Pal., *Cosmic Rays and their interactions*, 1966, 99.
13. Klebesadel R.W., Strong I.B., Olson R.A. et. al., *Astrophysics Journal*, L85 (1973) 182.
14. Smith G.R., Ogman M., Buller E. et. al., *Physical Review Letter*, 50(1983) 2110.
15. Hillas A.M., *Nature*, 50(1984)312.
16. Chakrabarti C., Bhadra A., Sarkar S.K. et. al., *Proc. of the 25th ICRC*, 1997, HE-6.1.8.
17. Hara T., Hayashida N., Ishikawa F. et. al., *Proc. of the 16th ICRC*, Kyoto, 11 (1979)166.
18. Bruce A., Denton J. et. al., *Proc. of the 17th ICRC*, Paris, 8 (1981)161.
19. Astley S.M. et. al., *Proc. of the 17th ICRC*, Paris, 9(1981)191.
20. Ng L.K. and Chan S.K., *Proc. of the 19th ICRC*, Lajolla, 7(1985)252.
21. Bhat P.N., John A.V., Upadhyaya S.S., *Nucl. Inst. Methods Phys Res. A. Accel*, 1990, Vol-A 292, No-2, 494-504.
22. Lu Y., Markeiewicz T. et. al., *Proc. of the 22nd ICRC*, Dublin, 4 (1991) 421.

23. Allen G.E., Barwick S. et. al., *Proc. of the 24th ICRC*, Rome, 1(1995)914.
24. Ammev S.S., Chasnikov I.Y. et. al., *Proc. of the 24th ICRC*, Rome, 1(1995) 66.
25. Mantash M.P., *FERMILAB Conf-96/007*, January 1996.
26. Hovjat C., *FERMILAB Conf-97/039*, GAP 97-021, February 1997.
27. Hovjat C., *FERMILAB Conf-97/071*, GAP 97-016, March 1997.
28. Catz Ph., Gawin J., Grochalska B. et. al., *Proc. of the 14th ICRC*, Munchen, 12 (1975)4329-4333.
29. Aliev N., Alimov T., Kakhaarov N. et. al., *Proc. of the 19th ICRC*, Lajolla, 7(1985)191.
30. Adamov D.S., Afanasjev B.N., Arabkin Y.V. et. al., *Proc. of the 20th ICRC*, Moscow, 5(1987)460.
31. Aglietta M., Alessandro B., Antonioli P. et. al., *Proc. of the 23rd ICRC*, Calgary, 4(1993)247.
32. Dedenko L.G. and Yakovlev V.I., *Proc. of the 23rd ICRC*, Calgary, 4(1993) 387.
33. Danilova E.V., Kabanova N.V. et. al., *Proc. of the 24th ICRC*, Rome, 1 (1995) 285.
34. Ter-Antonian S.V., Mamijanian E.A. et. al., *Proc. of the 24th ICRC*, Rome, 1 (1995) 365.
35. Asakimori K., Jogo N. et. al., *Journal of the Phys. Soc. of Japan* , 51(1982) 2059-2067.
36. Chan S.K. and Ng L.K., *Proc. of the 19th ICRC*, Lajolla, 7(1985)131-134.

Chapter-2

1. Klebesadel R.W., Strong I.B., Olson R.A. et. al., *Astrophysical Journal*, L85 (1973) 182.
2. Smith G.R., Ogman M., Buller E. et. al., *Physical Review Letter*, 50(1983)2110.
3. Hillas A.M., *Nature*, 50(1984)312.
4. Chakrabarti C., Bhadra A., Sarkar S.K. et. al., *Proc. of the 25th ICRC*, 1997, HE-6.1.8.
5. Basak D.K., Chakrabarty N., Ghosh B. et. al., *NIM*, 167(1984)227.
6. Basak D.K., Chaudhuri N., Sarkar S. et. al., *IL NUOVO CIMENTO* , 10C (1987) 169.

Chapter-3

1. Hillas A. M. and Lapikens J., *Proc. of the 15th ICRC*, Plovdiv, **8**(1997) 460.
2. Bassi P. et. al., *Phys. Rev.*, **92**(1953)441.
3. Linsley J. and Scarsi L., *Phys. Rev.*, **128**(1962)2384-2392.
4. Watson A.A., *Proc. of air shower workshop*, Utah, 1979,1.
5. Linsley J., *Journ. Phys., G, Nucl. Phys.*, **12**(1986)51.

Chapter-4

1. Catz Ph., Gawin J. et.al., *Proc. of the 14th ICRC*, Munchen, **12**(1975)4329.
2. Idenden D.W., *Proc. of the 21st ICRC*, Adelaide, **9**(1990)13.
3. Fenyves J., *Techniques in UHE g-ray astronomy*, ed. R.J. Protheroe and S.A. Stephens, University of Adelaide, 1985, 124.
4. Ciampa D. and Clay R.W., *Journ. Phys. G. Nucl. Phys.*, **14**(1988)787-792.
5. Galbraith W., *Extensive air shower*, 1958, p-99.
6. Galbraith W., *Extensive air shower*, 1958, p-114.
7. Galbraith W., *Extensive air shower*, 1958, p-124
8. Hodson L., *Proc. Phys. Soc.*, **A66**(1953)49,65.
9. Asakimori K., Jogo N., Kameda T. et. al., *Jorn. of the Phys. Soc. of Japan*, No.7, **51**(1982)2059-2067.
10. Atrashkevitch G.V. et. al., *Izv. Akad. Nauk. SSSR. Ser fiz.*, 1991, 55.
11. Ashton F. et.al., *Proc. of the 16th ICRC*, Kyoto, **13**(1979)243.
12. Hara T. et.al., *Proc. of the 16th ICRC*, Kyoto, **13**(1979)154.
13. Aglietta M. et. al., *Proc. of the 23rd ICRC*, Dublin, **4**(1993)247.
14. Danilova E.V. et al., *Proc. of the 24th ICRC*, Rome, **1**(1995)285.
15. Gerhardy P.R., Clay R.W. et. al., *Proc. of the 17th ICRC*, Paris, **6** (1981)162.
16. Tonwar S.C., *Proc. of the 17th ICRC*, Paris,1981, Rapporteur paper.
17. Trzuppek A., Lu Y. and Poirier J., *Proc. of the 23rd ICRC*, Calgary, **4**(1993) 359.
18. Simon P.S., *Proc. of the 24th ICRC*, Rome, **2**(1995)697-700.
19. Samorski M. and Stamm W., *ApJ Letters*, **L17**(1983)268.
20. Protheroe R.J., Clay R.W. and Gerhardy P.R., *ApJ letters*, **L47**(1984)280.
21. Hillas A.M., *Proc. of the 20th ICRC*, Moscow, **2**(1987)362.

22. Tonwar S.C. et. al., *ApJ Letters*, **L107**(1988)330.
23. Asakimori K., Maeda T., Misaki Y. et. al., *Proc. of the 18th ICRC*, Bangalore, **11**(1983)189-192.
24. Nagano M., Hara T., Hatano Y. et. al., *Journ. of the Phys. Soc. of Japan*, No.5, **53**(1984)1667-1681.
25. Greisen K., *Annu. Rev. Nucl. Sci.*, **10**(1960)63.
26. Sanyal S., Ghosh B. et. al., *Aust. J. of Physics*, **46**(1993)589.
27. Hara T., Hatano Y., Hayashida N. et. al., *Proc. of the 18th ICRC*, Bangalore, **11**(1983)272.
28. Capdevielle J. N. and Gawin J., *Journ of Physics, G, Nucl. Phys.*, **8**(1982)1317.

Chapter-5

1. Basak D.K., Chakraborti N., Ghosh B. et. al., *Nucl. Instrum. Methods*, **227** (1984) 167.
2. Trzupek A., Lu Y. and Poirier J., *Proc. of the 23rd ICRC*, Calgary, **4** (1993)359.
3. Kawamura Y. et. al., *Phys. Rev.*, **D40**(1989)729.
4. Ichimura M. et. al., *ICRR Report*, **287**(1992)92-95.
5. Blake P.R. and Tummev S.P., *Proc. of the 23rd ICRC*, Calgary, **4**(1993) 363.

A NEW DATA ACQUISITION SYSTEM FOR THE NBU EAS ARRAY.

C.Chakrabarti, A.Bhadra, S.K.Sarkar and N.Chaudhuri

High Energy and Cosmic Ray Research Centre, University of North Bengal, Dist. Darjeeling, INDIA 734430.

ABSTRACT:

A new data acquisition system developed for detection of Extensive Air Shower (EAS) events is described and the characteristics of the system relating to particle density measurement and particle arrival time measurement are presented.

Introduction:

The NBU Extensive Air Shower (EAS) array has been operating since 1980. Since the original construction of the array, a number of modifications and improvements have been made. The array currently consists of 24 scintillation detectors for the measurement of particle density of EAS at various points, 8 fast timing detectors for determination of the arrival direction of each shower event and two muon magnetic spectrographs for the study of muon component of EAS. One of the main purpose of the array is to search for discrete point sources of ultra high energy Cosmic Rays. For this a large air shower statistics is required which demands lowering of the shower size threshold of the array and small dead time of the data acquisition system. Moreover in a number of EAS observations it has been found that occasionally EAS are coming within short time interval (few ms.) (Klebesadel R.W. et. al., 1973, Smith G.R. et. al., 1983, Hillas A.M., 1984) having similarity with low energy gamma ray burst. To observe such phenomena, each shower event need to be recorded within few μ s. Considering these aspects, a new data acquisition system for the NBU EAS array has been developed. In the original data acquisition system of the NBU EAS array (Basak D.K. et. al., 1984) a 32 channel multiplexed ADC was used to digitised the analog pulse carrying the information of charged particle density in EAS. In the present system analog pulse heights are digitised simultaneously for all the 32 channels and these digitised density data and particle arrival time data are automatically recorded in an external 32 k-byte memory and subsequently stored in the Computer hard disk. In this paper the recording system, calibration of the read out system and instrumental errors are briefly described.

Recording System:

Fig-1 shows the schematic block diagram of the NBU EAS array data recording system. In the present form of the recording system, fast timing detector pulses are discriminated through a Lecroy discriminator. Discriminated output converted to TTL through Level adapter of Lecroy for coincidence. Out of eight fast timing detector we used three fixed and another one from remaining five for coincidence pulse generation.

The Particle Density Detector (PDD) pulses are amplified by an 'OPAMP' of gain 10 and the output is discriminated through a comparator to provide for a switching of time 4μ s. These pulses are also fed to a Sample and Hold (S/H) circuit. A hold pulse is generated from coincidence circuit. If a coincidence pulse comes within that 4μ s, the hold capacitor is isolated from discharging for a time of 150μ s. The output pulses of S/H are connected to the input of the Analog to Digital Converter (ADC) to scan the pulse heights. All the PDD channel scan these pulses simultaneously. The maximum time required to complete the scanning is 100μ s. There is a FET switch in each input of the S/H to disconnect the input channels from the S/H unit until the completion of total process. When a coincidence pulse is generated, a pulse of

width $150\mu\text{s}$ is fed to the ADC-Hold and a $1\mu\text{s}$ delayed pulse of width 150 nano second is generated in the coincidence circuit for the digital conversion of input analog pulse. We used a real time clock to get the shower arrival time and the date of individual shower.

Time to Digital Conversion (TDC) of fast timing detector pulse starts through a common start pulse of Lecroy model 2228A by a coincidence pulse. As common start comes, a capacitor is charged up by a constant current source until a stop pulse from an individual channel of fixed delay.

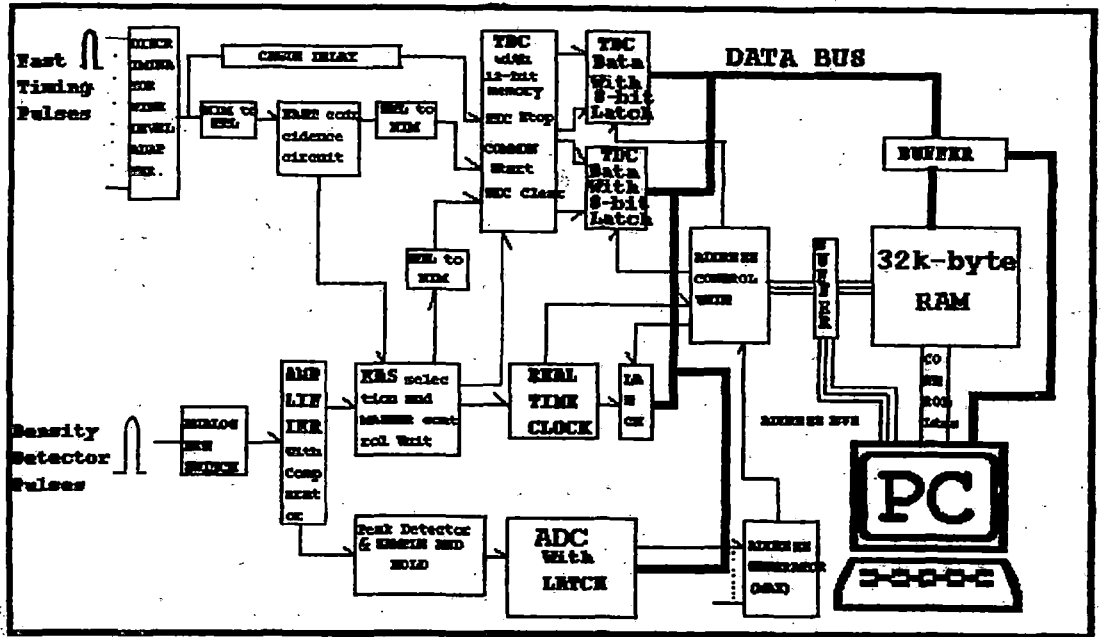


Fig-1. Block Diagram of the New Data Acquisition System.

When a coincidence pulse is generated, arrival time and date of the shower from the real time clock are stored into 8-bit latches and all the PDD data are stored into the individual ADC latch and 8-channel TDC data stored into TDC memory. After completion of these, a write pulse generated from the Master Control Unit (MCU) and an up counter of 15-address line start to increase the memory address for storing the data of arrival time, date, digital data of all PDD channels and the relative time difference for all TDC channels into the 32k-byte memory through 8-bit data bus.

The time between the arrival of individual shower and completion of data storage into the memory is about $200\mu\text{s}$. After $200\mu\text{s}$, the system is ready for the next event. The memory has nearly 1000 event data storing capacity. After completion of 1000 events, we start transfer all these data into the hard disk of a PC through parallel port. For the storage into hard disk from the external memory we use a software which is developed by us. The system has the provision to increase any number of PDD channels only by the addition of S/H and ADC.

Calibration of the Read Out System:

All the ADC are calibrated first using a standard dc source. In the next step a square wave pulse generator of variable amplitude was used as a standard source. The width of the pulses was taken comparable with the output analog pulses of the density detectors. Fig-2 shows an actual calibration

curve of a particular ADC. From the calibration curve it is found that digitised output pulses are linear to the input voltage upto 5 volt. The maximum error in ADC is 19.6 mv. The TDCs are calibrated using a standard timer.

Density Detector Calibration:

For the measurement of particle density, each density detector must be calibrated in terms of single particle pulse height. This was done by placing each scintillation detector within a telescopic arrangement of three G.M. counter, two of which were placed above the detector with their axis mutually perpendicular to each other and the third G.M. counter was placed below the detector. For the measurement of pulse height, the coincidence pulse from the telescope is used to trigger the MCU of the data acquisition system and the output from the detector is connected to each of the channels of the pulse height measuring circuit one after another. Most coincidences correspond to single particles. Fig-3 shows the single particle pulse height distribution of a particular detector. The Full Width at Half Maximum (FWHM) of single particle pulse height distribution for each of the channels is found to be within 27% of the average single particle pulse height of that channel.

During the operation of the array, the differential pulse height spectrum for all the detectors has also been measured sequentially and from the pulse height spectrum the average single particle pulse height was estimated.

Instrumental Uncertainty in Timing Measurements:

Instrumental uncertainty is measured in the following way. A coincidence of a vertical fast timing scintillation detector telescope is taken and this coincidence pulse starts TDC. Pulses of two detectors are fed to discriminator and the discriminated output pulses pass through with the same cable delay. These delayed pulses are used to stop the channels of the TDC. The distribution of the quantity $d = t_d - t_o + (d/c)$ is shown in Fig-4; where t_d is the time recorded by the lower detector, t_o is the time recorded by the upper detector, d is the vertical distance between the two detectors and c is the velocity of light. Assuming that the distribution is Gaussian, the standard deviation σ of the distribution gives the uncertainty in arrival time measurements and the uncertainty in timing measurement for a single detector is $\sigma/2^{0.5}$ which is (1.84 ± 0.05) nano second.

References:

1. Basak D.K., Chakrabarty N., Ghosh B. et. al., *NIM*, 167, 227 (1984)
2. Hillas A.M., *Nature*, 312, 50 (1984)
3. Klebesadel R.W., Strong I.B., Olson R.A. et. al., *ApJ*, 182, L85 (1973)
4. Smith G.R., Ogmen M., Buller E. et. al., *PRL*, 50, 2110 (1983)

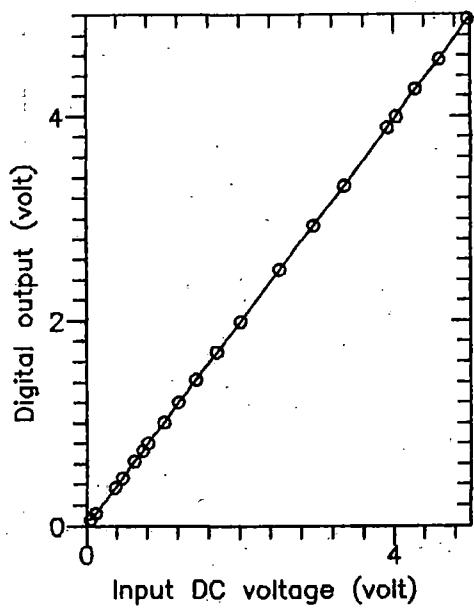


Fig-2. ADC Calibration.

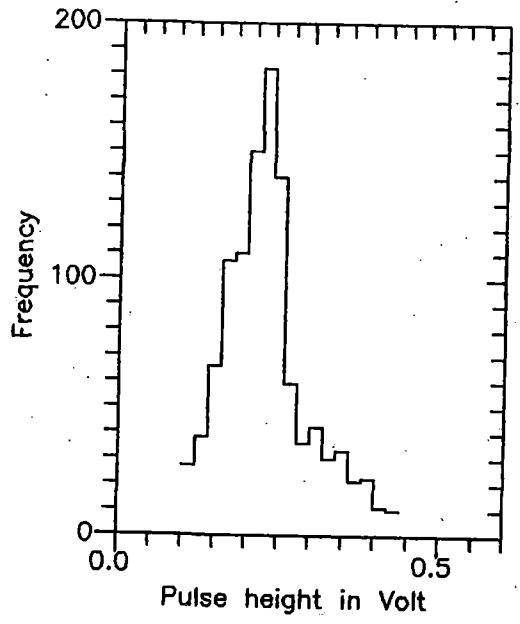


Fig-3. Single Particle Pulse Height Distribution.

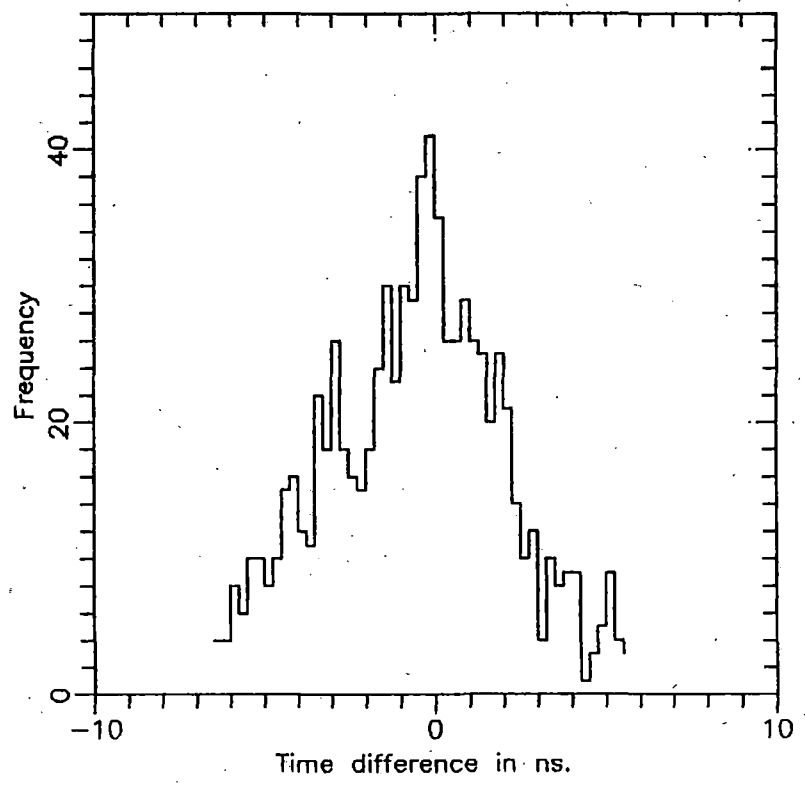


Fig-4. Instrumental Uncertainty in Timing Measurements.

The Zenith Angle Dependence of Shower Age

A. Bhadra, C. Chakrabarty, G. Saha and N. Chaudhuri

High Energy & Cosmic Ray Research Centre, University of North Bengal, Dist. Darjeeling INDIA 734430

ABSTRACT

The variation of shower age parameter with zenith angle for different shower size ranges is studied. The observed variation is in agreement with the electron-photon cascade theory and with the other EAS observations. It is found that upto zenith angle 30° , shower 'age' is practically independent of zenith angle. So it is difficult to correlate the observed high 'age' value of the directional excess showers with zenith angle.

Introduction

The longitudinal development of Cosmic Ray Extensive Air Shower (EAS) is an essential feature that reflects the gross feature of particle interaction at high energies. The stage of development of an air shower is described by shower age parameter (s). Showers that develop early in the atmosphere have on the average larger 'age' than late developing showers of equal primary energy. Discrimination of gamma-ray initiated showers from the large background of charged cosmic ray initiated showers based on shower 'age' has been used in several observations (Samorski and Stamm 1983; Protheroe et al 1984) on the assumption that, for same shower size, photon induced showers are older. But the Monte Carlo simulation results (Fenyves 1985, Hillas 1987, Cheung and Mackeown 1988) show that in 'age' the gamma-ray induced showers are not older than that of normal showers, though in several observations it is found that the excess showers from the direction of discrete point sources are characterised by high 'shower age' value (Samorski and Stamm 1983, Protheroe et al 1984, Fouin et al 1987, Tonwar et al 1988). In most of the observations the showers from point sources were observed at large angles during most of the observation time due to high angle of transit of the sources at the arrays. As for example, Cygnus X-3 is observed at Kiel at zenith about 14° , the same source is observed at Ooty at zenith angle nearly 26° at the transit. Though in the search for evidence of UHE emission the source and background events are collected during the same time in the same zenith angle intervals still there is a remote possibility (because of small statistics) that the source events had higher zenith angle than the background events. And with the increase of zenith angle the atmospheric thickness increases, so showers with high zenith angles are expected to have high shower 'age' values. To better understand the problem in the present work the dependence of shower age on zenith angle in the range $0^\circ - 55^\circ$ for three different shower size range is examined.

Experimental Set-up :

The air shower array at North Bengal University campus (latitude $26^\circ 42'$ N, longitude $88^\circ 21'$ E, 150 m a.s.l.), INDIA, is operating since 1980. At present it is composed of twenty four plastic scintillation counters, each of area 0.25 m^2 , for the measurement of particle density of air shower, eight fast timing detectors, each having also an area of 0.25 m^2 , for the determination of the arrival direction of the air showers. Two magnet spectrographs of maximum detectable momentum 220 GeV/c, each of an area 0.25 m^2 , under a concrete shielding absorber are also operated in conjunction with the air shower array for the study of muon component of EAS. Each spectrograph consists of a solid iron magnet in between four neon flash tube trays (used as muon track detector). The effective shower size threshold for the array is 2×10^4 particles. Details of the

experimental system and data acquisition are described elsewhere (Basak et al 1984, Bhadra 1996, Chakrabarty et al 1997).

Data Analysis :

The recorded showers have been analysed for core position (X_o, Y_o), shower size (N_e), shower age (s) and arrival direction (l, m, n). Shower size, shower age and core position were determined by a least square fit of observed particle density to NKG (Greisen 1960) lateral distribution. Showers with cores landing within 30 m from the centre of the array (approximately the array boundary) were only accepted. The resolution of the core position is ± 2.8 m and that of shower age and shower size are ± 0.11 and $\pm 17\%$ respectively (Bhadra 1996).

The arrival direction were obtained by measuring the relative arrival times (t) of the shower particles at different points. Using conical shower front and radial distance dependent weight factors the arrival direction of each shower event was calculated by a least square fit to the timing data. Deviation from the plane shower front was taken through the empirical equation (as measured by the array, Bhadra 1996)

$$dt = 0.19 r - 2.12$$

To incorporate the variation of shower front thickness with core distance the weight factor used in the analysis is given by

$$w_i = 1/(\sigma_t^2 + \sigma_{inst}^2)$$

where σ_t is the spread of the arrival of the shower front particles and was taken as (Linsley 1986)

$$\sigma_t = \sigma_o / \sqrt{n} (1 + r/r_t)^b$$

with $\sigma_o = 1.6$ ns, $r_t = 30$ m and $b = 1.65$, n is the number of particles that hit the detector. σ_{inst} is the instrumental error of the timing detector. Instrumental uncertainty of the timing detectors of the array was found around 1.25 ns.

The angular resolution of the array has been estimated by the conventional 'split the array' method and is nearly 1.1° in zenith.

Results :

The results of the present work are based on a sample of nearly 10000 EAS events which were collected by the array during Jan 1994 to June 1994. The general features of the EAS (e.g. lateral distributions of electrons and muons, shower age distribution, $N_\mu - N_e$ relation etc.) observed by the array were reported earlier (Basak et al 1987, Sarkar et al 1991, Bhadra 1996) and are consistent with the well known characteristics of air showers.

The age distribution of the observed showers for the showers in the size range $6 \times 10^4 < N_e < 1 \times 10^6$ is shown in fig 1. The mean age of the observed showers is 1.31 which is close to the theoretical estimate (1.33 for proton showers) of Fenyves(1985) but differs with $s = 1.45$ measured at Haverah Park (Idenden 1990) and $s = 1.1$ measured at Kiel (Samorski 1983) at the same observation level. The zenith angle distribution of the observed showers in the same shower size range is given in figure 2. The peak of the distribution is observed at around 20° .

The variation of mean shower 'age' with zenith angle for three shower size range, $(7.5 - 8.5) \times 10^4$, $(1.5 - 2.5) \times 10^5$ and $(5.5 - 6.5) \times 10^5$, are shown in figure 3. The Figure shows that the nature of the variation does not vary much with shower size. The variation of s with zenith angle (z) is found slow and up to zenith angle 30° the shower age is practically found to be independent of zenith angle. In the shower size range $(1.5 - 2.5) \times 10^5$ the mean shower age is 1.29 at $z = 2.5^\circ$ and at $z = 52.5^\circ$ the mean 'age' reaches only 1.44 though at zenith angle 52.5° the atmospheric overburden is nearly double. The observed variation can be expressed by the relation

$$s = s_o + A \text{Sec}(z) \quad \dots\dots\dots(1)$$

where the value of s_o and A for different shower size range are given in table 1.

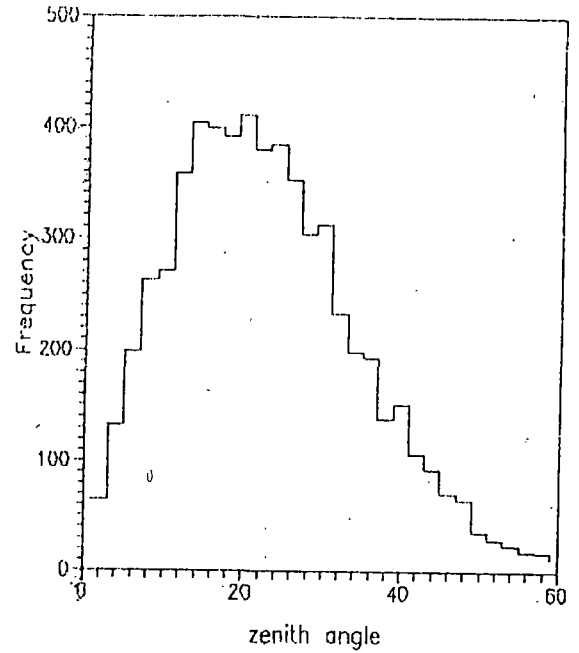
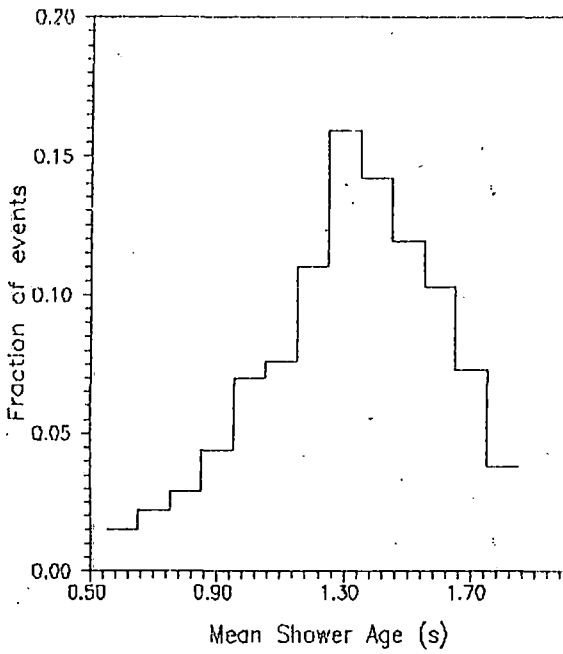


Fig. 1. Age distribution of the observed showers

Fig. 2. Zenith angle distribution of the observed Showers

The development of electron-photon cascade is approximately described by the equations (Greisen 1960)

$$s = 3t/(t + 2w) \quad \dots\dots (2)$$

and
$$N_e = (0.31/\sqrt{w}) \exp[t (1 - 1.5 \ln s)] \quad \dots\dots (3)$$

where $w = \ln E/\epsilon_0$ and t is the atmospheric depth in radiation length . Using eqns (2) and (3) and expressing the variation of s with z for three different shower size range through the relation as given in eqn.(1) the values of s_0 and Λ for different N_e are also given in table (1). The result shows that the observed variation is in accordance with the cascade theory .

Table 1. Comparison of the observed variation of age parameter with zenith angle with the cascade theory for three different shower sizes.

N_e		8×10^4	2×10^5	6×10^5
Observed	s_0	1.10	1.03	0.98
	Λ	0.22	0.26	0.27
Theory	s_0	1.15	1.11	1.05
	Λ	0.27	0.28	0.30

Discussion :

Present result of the variation of shower age with zenith angle agrees with the prediction of cascade theory . In a number of EAS observations (Aguirre et al 1973, Miyaki et al 1981, Clay et al 1981 ,Idenden 1990) similar trend of variation was observed . In the Kiel observations, showers with zenith angle less than 30° only were accepted for the analysis . So it is difficult to correlate the high 'age' value of the directional excess showers with zenith angle.

Acknowledgements : We are thankful to Dr.B.Ghosh , Dr.S.K.Sarkar , Dr. S.Sanyal , Mr. A.Mukherjee and Mr.A.Chettri for their help in operation of the array .

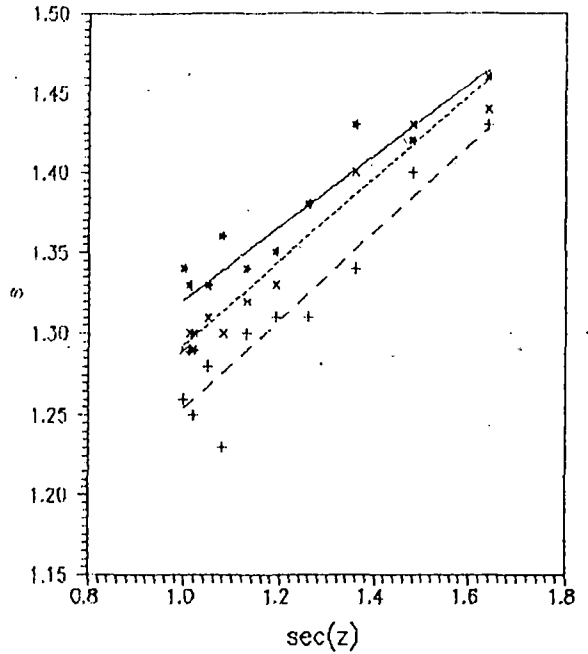


Fig. 3. Variation of shower age with zenith angle for three different shower size range (* -- $N_e = (7.5 - 8.5) \times 10^4$, x -- $N_e = (1.5 - 2.5) \times 10^5$, + -- $N_e = (5.5 - 6.5) \times 10^5$.

References :

- Aguirre ,C. et al , *Proc. 13 th ICRC (Denver)* , 4 , 2598 (1973)
 Basak , D.K. , Chakrabarty , N. , Ghosh , B. , et al , *Nucl. Instrum. Methods* 227 , 167 (1984)
 Basak , D.K. , Chaudhuri,N. , Sarkar , S. , et al , *IL Nuovo Cimento* , 10 , 169 ,(1987)
 Bhadra , A. , *Ph.D. thesis , University of North Bengal (Unpublished)* , (1996)
 Chakrabarty ,C. , Bhadra , A. , Sarkar , S.K. , and Chaudhuri ,N. , *Proc. 25 th ICRC* , HE2.6(1997)
 Cheung , T. and Mackeown ,P.K. , *IL Nuovo Cimento* , 11C , 193 (1988)
 Clay , R.W. , Gerhardy , P.R. , Liebing , D.F. et al , *IL Nuovo Cimento* , 4C , 668 (1981)
 Fenyves , J. , *Techniques in UHE γ -ray astronomy* , ed. R.J.Protheroe and S.A.Stephens , University of Adelaide , 124 (1985)
 Fomin , Yu.A.et al , *Proc 20th ICRC* , Moscow , 1 , 397 (1987)
 Greisen , K. , *Annu. Rev. Nucl. Sci.* , 10,63(1960)
 Hillas ,A.M. , *Proc 20th ICRC* ,(Moscow) , 2 , 362 (1987)
 Idenden , D.W. , *Proc. 21st ICRC (Adelaide)* , 9 , 13 (1990)
 Linsley , J. , *J.Phys.G : Nucl. Phys.* , 12 . 51(1986)
 Miyaki , S. , Ito , N. , Kawakami , S. , Hayashi , Y. , *Proc. 17th ICRC* , 11 , 293 (1981)
 Protheroe , R.J. , Clay , R.W. , and Gerhardy , P.R. , *Ap.J. Lett.* 280 , L47 (1984)
 Samorski , M. , and Stamm ,W. , *Ap J (Lett)* , 268 , L17 (1983)
 Sarkar , S.K. , Ghosh , B. , Mukherjee N. , et al . *J.Phys. G:Nucl Part Phys.* , 17 , 1279 (1991)
 Tonwar , S.C. , et al , *Ap.J. Lett.* 330 . 107 (1988)

Study of electrons simultaneously with muons in
Extensive Air Showers (EAS) initiated by Primary
Cosmic Rays of energy 10^{14} - 10^{16} eV

C. Chakrabarti, D. Chanda, G. Saha, A. Mukherjee, A. Bhadra
S. Sanyal, S. K. Sarkar, B. Ghosh, N. Chaudhuri.
High Energy & Cosmic Ray Centre.
North Bengal University
Darjeeling, India

Abstract.

An air shower experiment performed with the provision of direct measurement of both low and high energy muons simultaneously by magnet-spectrographs has yielded radial muon density distributions at various measured muon energies and radial electron density distributions as a function of known shower size of measured age. The characteristics of these distributions in terms of the measured shower parameters have been determined to draw conclusions about the mass of the primaries of EAS.

1.- Introduction:

The initial results of the first set of measurements of both the electron and muon distributions in EAS in the size range 10^4 - 10^6 particles (primary energy range 2.2×10^{14} - 4.8×10^{15} eV) have been presented in the previous ICRC sessions (1983, 1985, 1987, 1990) by the NBU group. The direct measurements of muon energies by two magnet-spectrographs of the NBU EAS array provide accurate data to form a base for comparison with the predictions of different EAS models for various primary compositions. The present report presents the final results of our first experiment.

2.- Method:

The method was same as we described in previous reports (1983, 1985, 1987, 1990). The magnet-spectrographs for recording muons were operated in coincidence with the EAS array of particle density detectors and timing detectors under a fixed set of selection criteria. The average electron and muon densities in each of various narrow shower size bins in the

shower size range 10^4 - 10^6 particles was obtained as a function of r and muon energy E_μ (not exceeding E_{μ}). These results yield radial distributions for muon density with energy not exceeding E_μ as well as the muon energy spectrum at various muon distances r over the range 0-120 m .

3.-Results:

3.1:-The measured muon energy spectrum.

The muon energy spectra have been measured for various average shower sizes. For average shower size $\bar{N}_e = 2.2 \times 10^4$ particles ($\bar{s} = 1.25$) in the radial range 0-100 m the muon energy spectrum fits to :

$$N_\mu(>E_\mu) \sim E_\mu^{-\alpha_\mu(r)} \quad \text{--- (1)}$$

where $\alpha_\mu(r)$ changes from 0.26 at about 5 m to 1.01 at about 90 m showing the degree of dependence of energy spectrum of muons on the distances from the EAS axis .

3.2:-Muon density dependence on average shower size \bar{N}_e .

For different threshold muon energies and the radial distances from the EAS axis, the results of muon density dependence on shower size fit to :

$$\rho_\mu(>E_\mu, r) \sim \bar{N}_e^\beta(E_\mu, r) \quad \text{--- (2)}$$

The exponent β is weakly dependent on r and the threshold muon energy E_μ . For example for muons of energy exceeding 10 GeV at r between 16 and 32 m, the value of β is 0.72 whereas for $E_\mu > 100$ GeV for the same value of r between 16 and 32 m, the value of β is 0.68 .

It is further seen (fig.1) that for low energy muons in showers of size less than $10^{5.25}$ particles the exponent β decreases with r increasing whereas in larger showers of size greater than $10^{5.25}$ particles, β increases with r . For high energy muons β decreases with r in showers of size below and above $10^{5.25}$ particles. At different radial distances and for different low muon threshold energies β changes around the shower size $10^{5.25}$ particles. Such variation of β implies that the muon radial distribution function changes with the primary energy. The measured muon

lateral distribution for each shower size and muon energy exceeding E_{μ} in the radial range between 0 and 120 m shows a fit to the form

$$\rho_{\mu}(\geq E_{\mu}, r, N_e) \sim r^{-k(\geq E_{\mu})} \exp(-r/r_0) \quad \text{--- (3)}$$

This shows that the muon lateral distribution function depends on muon energy threshold. The exponent k has the values in the range 0.26 - 1.22 .

The measured data of muon density also fit to a single parameter form :

$$\rho_{\mu}(\geq E_{\mu}, r, N_e) \sim r^{-\alpha(\geq E_{\mu})} \quad \text{--- (4)}$$

values of α within an error range 8-10 % from the fit of the data for $E_{\mu} \geq 2.5$ GeV. are shown as a function of N_e in fig.2 . The trend of α vs. E_0 (the conversion of shower size to primary energy E_0 is in accordance with the energy scaling factor of Aliev et. al. [1] and Trzuppek et. al. [2]) curve shows that α is a function of energy up to 2×10^{15} eV and becomes constant at higher energies. Such a variation of α with E_0 implies that the effective primary mass is decreasing with increasing energy over the range 10^{14} - 10^{15} eV and becomes constant at higher energies.

3.3-Radial distribution of electrons compared with radial distribution of muons:

The radial muon density distribution in young developing showers ($s \leq 1.0$) as well as in old decaying showers ($s \geq 1.0$) is flatter compared to the radial electron density distribution which is shown in fig.3 for $N_e = 3.3 \times 10^5$. The muon densities in old showers are high than those in younger showers of the same size by a factor two.

4.-Discussion.

The properties of the measured radial distribution of muon density in EAS as a function of primary energy in the range 10^{14} - 10^{15} eV indicate continuously decreasing primary mass composition. The measured value and shape of the radial distribution for muons and electrons at small and large distances from the EAS axis are similar to the Monte Carlo results obtained for primary proton initiated EAS (Poirier et al. [3])

References

- [1] Aliev N et al 19th ICRC 7(1985)191
- [2] Trzupcek A. et al 23rd ICRC 4(1993)359
- [3] Poirier J. Gress J. Mikocki S. et al ICRC 9(1990)126

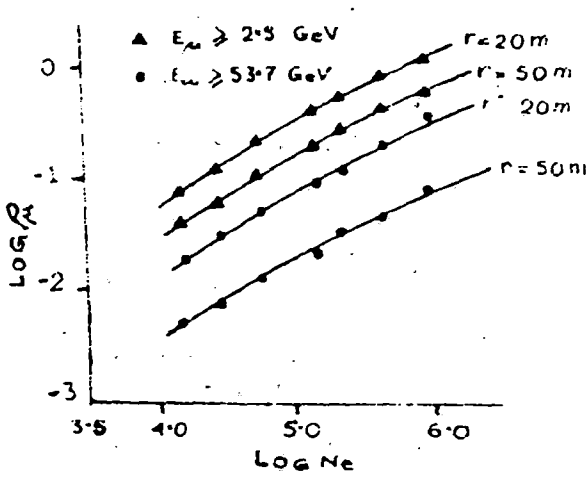


Fig 1

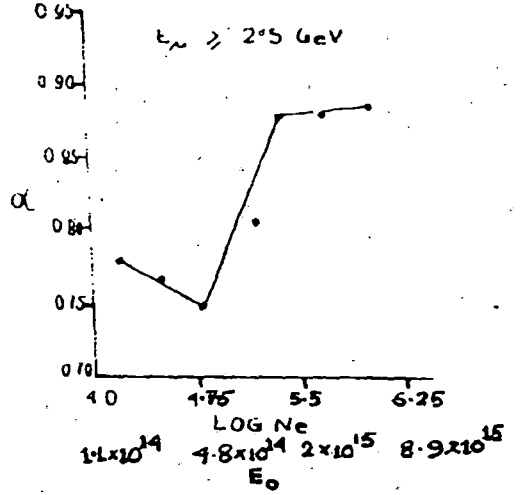


Fig 2

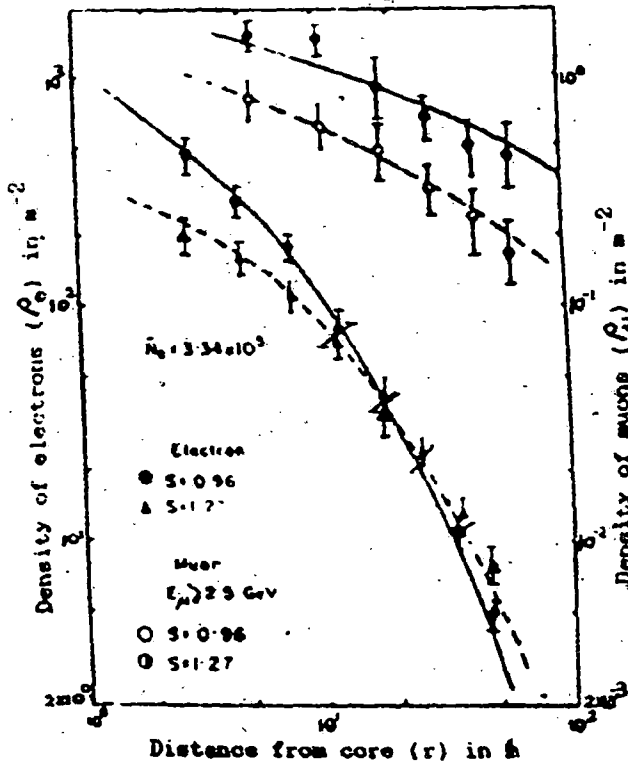


Fig 3

Figure Captions :

Fig.1. Variation of muon density at radial distances 20 m & 50 m with shower size (vertical showers) at $E_{\mu} \geq 2.5$ & 53.7 GeV

Fig.2. Variation of α with N_e at $E_{\mu} \geq 2.5$ GeV

Fig.3. Electron and muon lateral density distributions for old decaying and young developing vertical showers.

Low And High Energy Muons In Extensive Air
Showers Of Size 10^4 To 10^6 Particles

C. Chakrabarti, D. Chanda, G. Saha, A. Mukherjee,
A. Bhadra, S. Sanyal, R. K. Chhetri, S. K. Sarkar,
B. Ghosh and N. Chaudhuri.

High Energy and Cosmic Ray Center
North Bengal University
Darjeeling
India-734 430

Abstract

Accurately measured energy spectra and radial distributions of low and high energy muons in Extensive Air Showers (EAS) are presented and compared with Monte Carlo calculations assuming specific hadronic interaction characteristics of primary protons with air nuclei in the primary energy range 2.2×10^{14} - 4.8×10^{15} eV.

I-Introduction:

Knowledge of radial distribution together with energy distribution of muons in EAS is of fundamental importance as such data have explicit energy dependence and are expected to be sensitive to both the primary cosmic ray composition and the characteristics of hadronic interaction with air nuclei.

This paper contains accurately measured data on low and high energy muons detected in association with EAS at sea level. By direct and accurate measurement of muon energy over a wide range of energy and radial distance from the EAS axis, the present experiment provides a firmer base for comparing with the theoretical predictions for different primary compositions.

II-Experiment and Method:

The experimental set up consists of an air shower array of 32 electron detectors and two

magnet spectrographs for recording and measuring muon momenta accurately in association with individual EAS incident on the array. The description of the array system and spectrographs was given by Basak et al. (1). Low and high energy muons in the range of 2.5 - 200 GeV in EAS of size 10^4 to 10^6 particles (primary energy range 2.2×10^{14} - 4.8×10^{15} eV, determined by using the energy scaling factor of N. Aliev et al. (2) and A. Trzupsek et al. (3)) were recorded by the two spectrographs simultaneously with the recording of the EAS events by the array. The EAS parameters such as shower size (N_e), age parameter (s), EAS axis location and the radial distance of each recorded muon were determined by the method of least squares.

The recorded muon deflection angle is converted to incident momentum of muon (momentum resolution of spectrograph 17% to 38% for energy range 2.5 - 200 GeV) by the method described by Basak et al. (1). The density of muons of energies above a threshold value in EAS of measured parameters was determined as a function of muon radial distance from the shower core.

III-Results:

Some of the representative experimental data, with typical poissonian error on a few points only, in the form of muon lateral distribution for a fixed shower size at different threshold energies (fig.1), muon energy spectrum at a fixed radial distance for two different shower sizes (fig.2) and the variation of muon density with average shower size with threshold muon energy of 2.5 GeV at two different radial distances from the shower core (fig.3) are shown.

A comparison of the measured electron lateral distribution (fig.4), muon lateral distribution (threshold energy 2.5 GeV) (fig.5) and the ratio of muon and electron density for different shower sizes (fig.6) with data calculated by Monte Carlo simulation of Poirier et al. (4) utilising simulation codes SHOWERSIM (model WOO) and EGS for proton primaries is also given. The hadron-hadron interaction model WOO (details presented by Mikocki et al. (5)) has scaling behaviour below 1 TeV but at higher energies the

scaling is mildly violated in the fragmentation region and significantly violated in the central region. The hadron-air interaction cross section and the multiplicity of pions and kaons increase with energy but the inelasticity distribution ($1/2$ for nucleons and $2/3$ for mesons) and the transverse momentum distribution (325 MeV/c for pions and 371 MeV/c for kaons) are independent of energy.

Discussion:

The present measurements of energy spectra and radial distributions of muons do not provide any evidence for heavy primaries (in the primary energy range 2.2×10^{14} - 4.8×10^{15} eV). The hadronic interaction characteristics assumed in the above mentioned model are found to be consistent with the measured data upto the fixed shower size of 10^5 particles. Using the same hadronic interaction characteristics the shape of the muon density distribution in primary iron initiated EAS is similar to that for proton initiated shower with the same primary energy but the magnitude of the distribution is higher for low energy muons in the vicinity of the EAS core (0 to 100 meter). The present experiment does not find such features in the observed muon data. The measured electron lateral distribution is in good agreement with the calculated distribution but the measured muon lateral distribution is much broader than the calculated. The same feature can be seen in the density ratio distribution (fig.6) which also shows that both the measured and calculated ratio exceeds unity beyond the distance of 100 meter from the core.

References:

1. Basak D.K. et al.
Nucl. Inst. Methods Phys. Res., 227, (1984), 167.
2. Aliev N. et al.
19th ICRC (La Jolla, 1985), 7, 191.
3. Trzupsek A. et al.
23rd ICRC (Calgary, 1993), 4, 359
4. Poirier J., Gress J. and Mikocki S.
21st ICRC (Adelaide, 1990), 2, 126
5. Mikocki S. et al., J. of Phys. G 13 (1987), L85

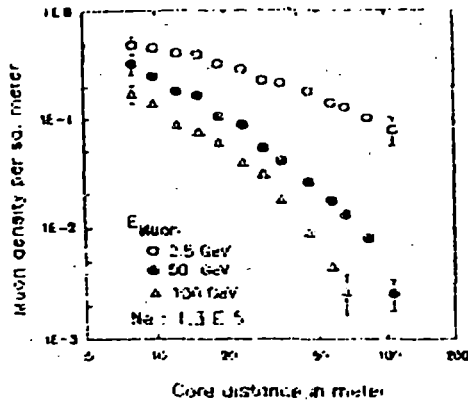


Fig. 1 Muon lateral distribution.

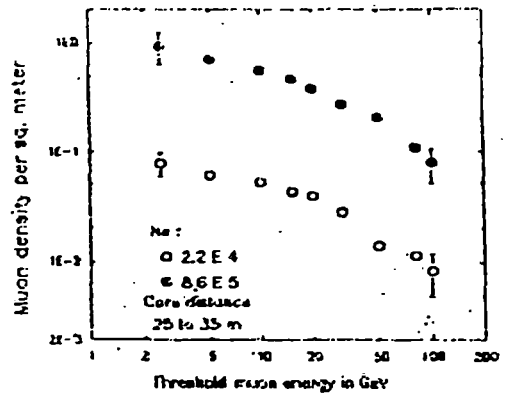


Fig. 2 Muon energy spectrum

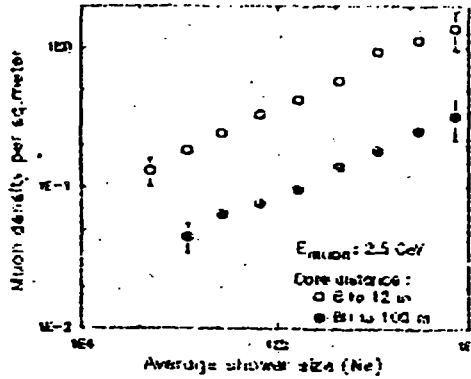


Fig. 3 Muon density and Ne distribution

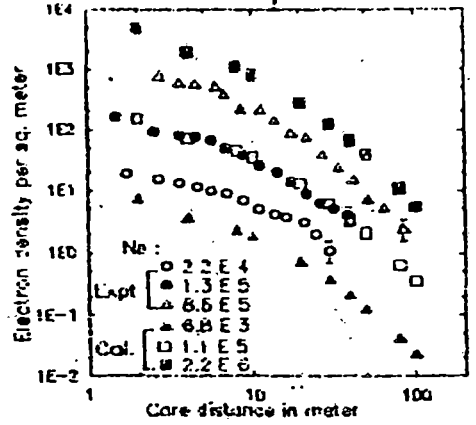


Fig. 4 Electron lateral distribution

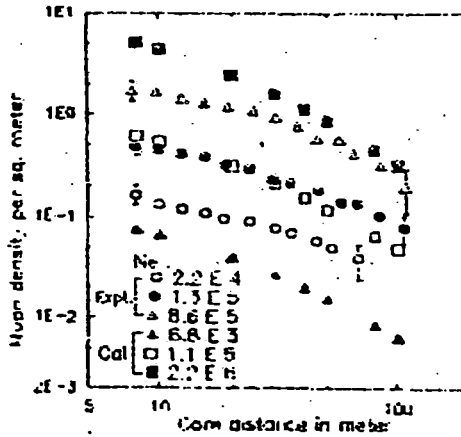


Fig. 5 Muon lateral distribution

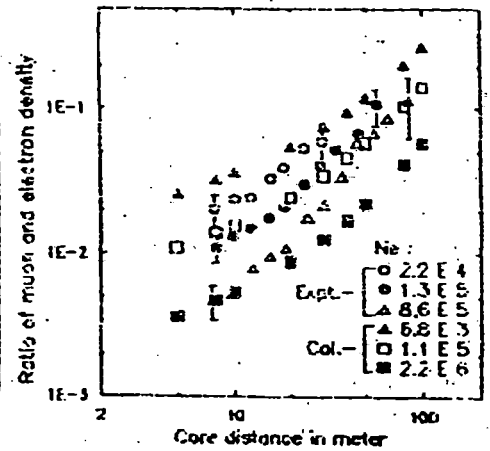


Fig. 6 Density ratio distribution

A SEARCH FOR ANISOTROPY IN THE ARRIVAL DIRECTION
OF EAS BY COSMIC RAYS FROM DISCRETE SOURCES

C. Chakrabarti, D. Chanda, G. Saha, A. Mukherjee,
A. Bhadra, S. Sanyal, R. Chettri, S. K. Sarker,
B. Ghosh and N. Chaudhuri

High Energy & Cosmic Ray Centre
North Bengal University (NBU)
Darjeeling 734430, INDIA

ABSTRACT

The NBU Cosmic Ray Telescope consisting of an EAS array of scintillation detectors and two magnet spectrographs has been operated in a search for any anisotropy in the directions of arrival of EAS events. The shower arrival directions are determined by fitting the measured shower particle arrival times. Initial results on distribution of events in declination and right ascension are given.

Introduction : A cosmic ray air shower telescope has been installed at a new location (latitude $26^{\circ}42' N$, longitude $88^{\circ}21' E$) to look for any anisotropy in the directional intensity of primary cosmic rays in the energy range 10^{14} - 10^{16} eV. The set up consisting of plastic scintillation detectors for electrons, two shielded magnet spectrographs for muons and eight fast timing scintillation detectors for shower particles arrival time measurements has been in operation for some time now. Preliminary results from the measurements of shower arrival directions are presented in this report.

Method of analysis : Some 13 thousands EAS events have been registered by the EAS array so far. For each event the shower parameters : the shower size (N_e), the shower age (S) and the shower core location (X_0, Y_0) have been determined using a fitting function to fit the measured electron density data by an iterative procedure for minimizing chisquare using gradient search method. The analysis on a selected group of showers in the size range $10^{4.3}$ - $10^{6.2}$ has led to

the following error estimates:

- (i) core location error is within ± 1 m,
- (ii) shower size error is $\pm 0.1 N_e$,
- (iii) age parameter error is within ± 0.06 .

The arrival direction of the shower is determined from the measured relative arrival time delay data by minimizing the quantity,

$$\chi^2 = W_i [lx_i + my_i + nz_i + c(t_i - t_0)]^2,$$

where t_i is the actual time measured by the i th detector, W_i is the statistical weight factor, c is the velocity of the EAS front which passes through the origin at t_0 and l, m, n are the direction cosines of arrival.

From the best fitted values of direction cosines the direction of arrival of each EAS event has been determined in local coordinate system (zenith angle, azimuth angle). Finally the EAS arrival direction angles are transformed into right ascension (α) and declination (δ). The resolution of the EAS array has been determined by the divided array method using those events in which all the timing detectors yielded information about the arrival time of the EAS front. The systematic and statistical uncertainties in the measurement of arrival direction have been determined and taken into account in the analysis. The estimated resolutions are 1.1° in declination and 1.6° in right ascension.

Results : Preliminary results from a small sample of shower arrival time data are given. The measured data on resolution of the EAS array are given in figures 1 and 2. The distribution of all the EAS events in declination (δ) is given in figure 3. The observed declination range is within -40° and $+88^\circ$ with a peak at $32^\circ - 34^\circ$ bin. Similar declination distribution of Mitsuishi EAS data (Fujita et al., 1993) showed a peak within $30^\circ - 40^\circ$. The right ascension (α) distribution is shown in figure 4. This distribution in right ascension has not been corrected for any effect arising out of occasional discontinuities in running time.

Reference :

Fujita K. et al, Proc. 23rd ICRC, Calgary, 1(1993)376

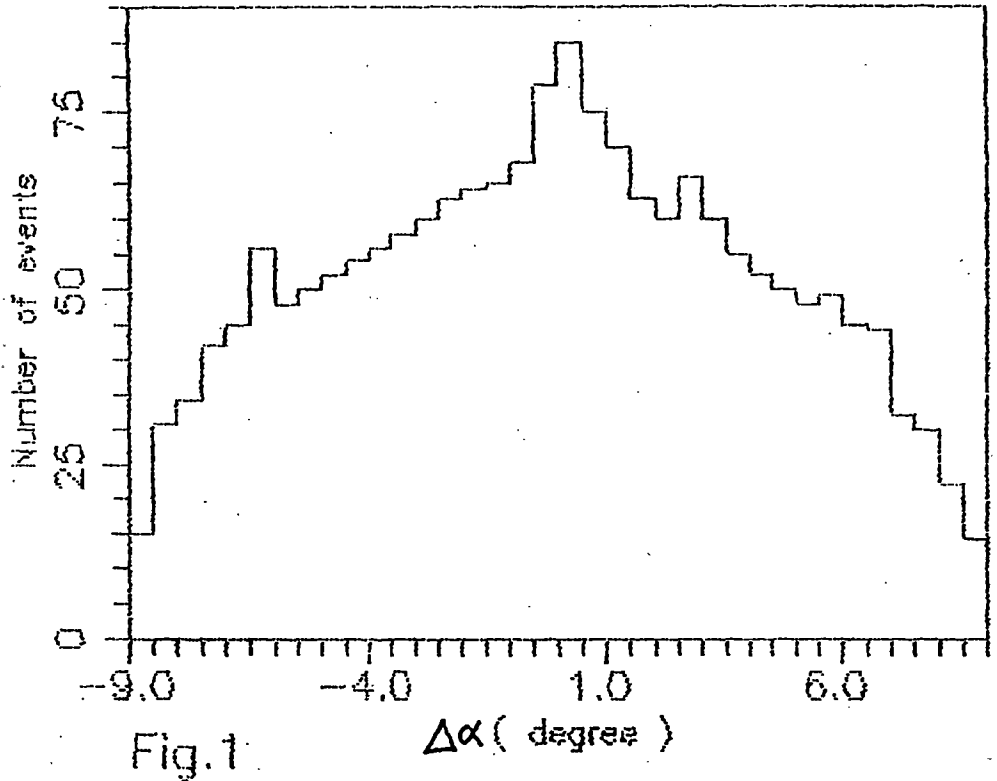


Fig.1

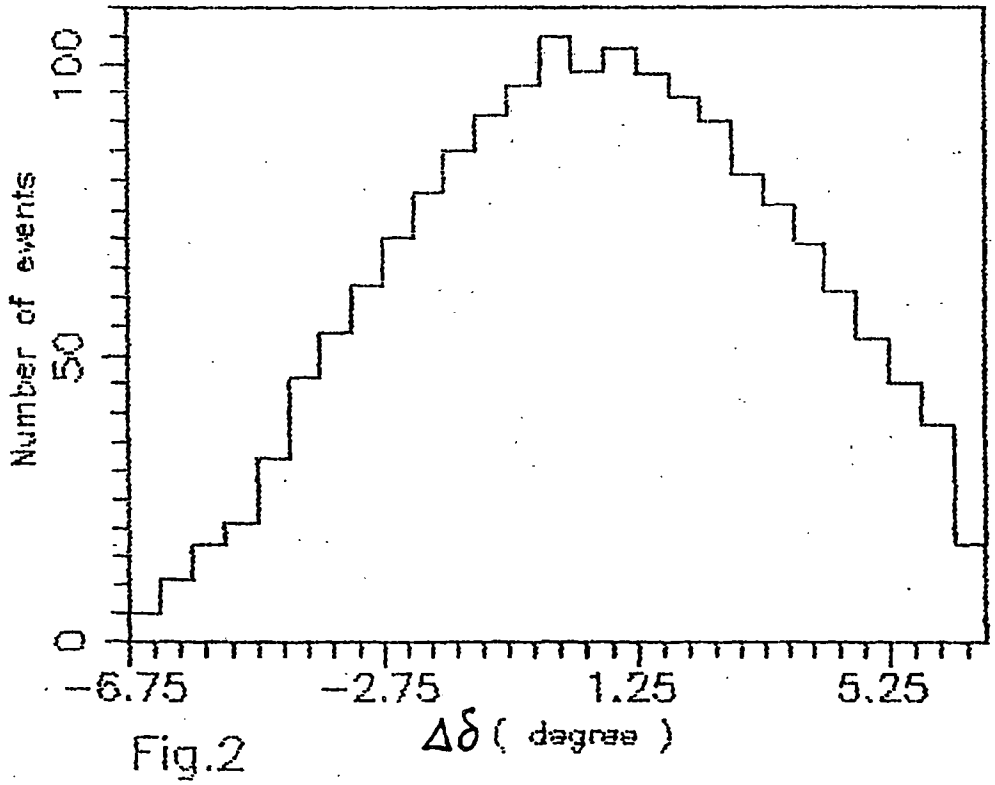


Fig.2

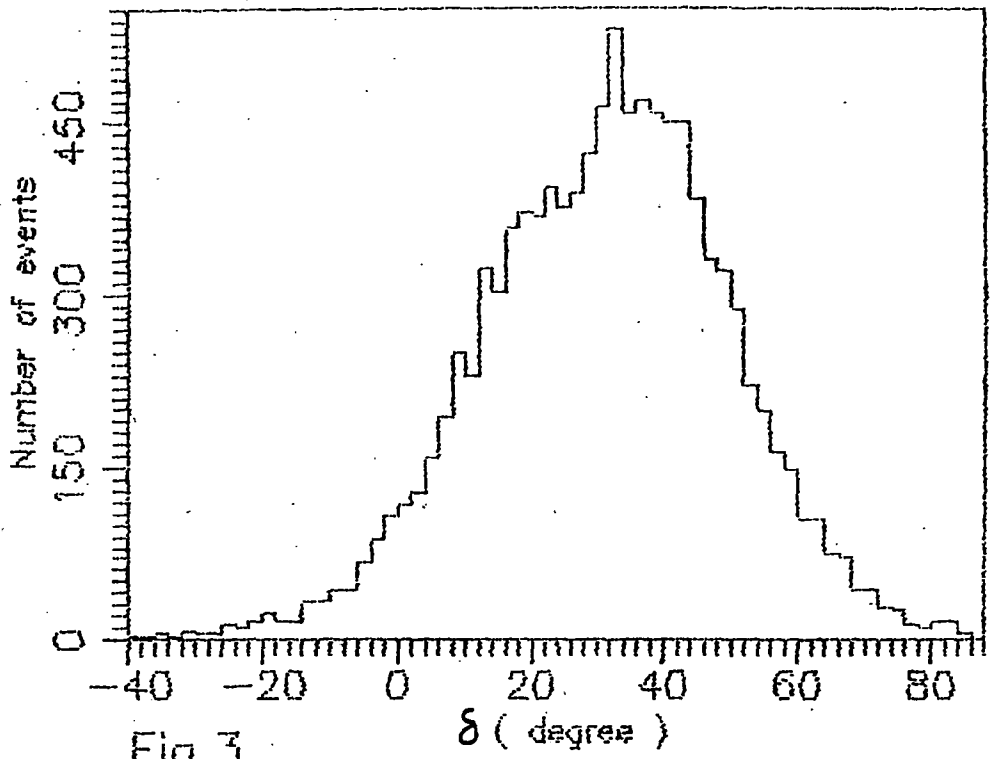


Fig.3

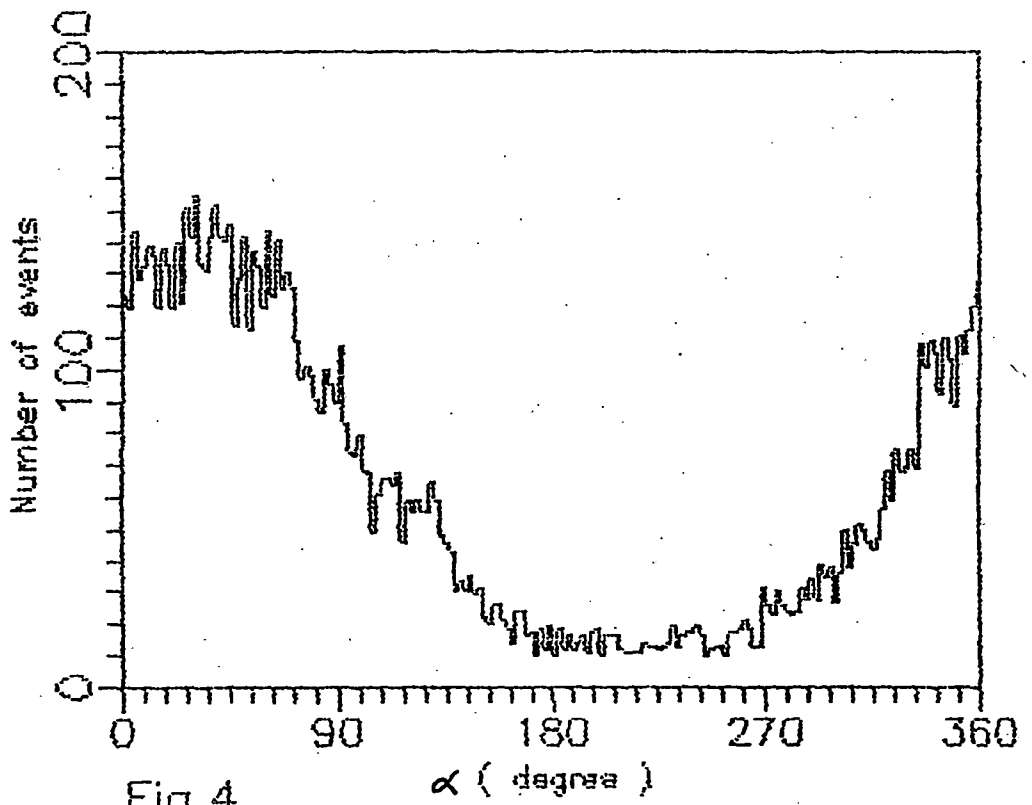


Fig.4

1980
 1981
 1982
 1983
 1984
 1985
 1986
 1987
 1988
 1989
 1990
 1991
 1992
 1993
 1994
 1995
 1996
 1997
 1998
 1999
 2000
 2001
 2002
 2003
 2004
 2005
 2006
 2007
 2008
 2009
 2010
 2011
 2012
 2013
 2014
 2015
 2016
 2017
 2018
 2019
 2020
 2021
 2022
 2023
 2024
 2025
 2026
 2027
 2028
 2029
 2030
 2031
 2032
 2033
 2034
 2035
 2036
 2037
 2038
 2039
 2040
 2041
 2042
 2043
 2044
 2045
 2046
 2047
 2048
 2049
 2050
 2051
 2052
 2053
 2054
 2055
 2056
 2057
 2058
 2059
 2060
 2061
 2062
 2063
 2064
 2065
 2066
 2067
 2068
 2069
 2070
 2071
 2072
 2073
 2074
 2075
 2076
 2077
 2078
 2079
 2080
 2081
 2082
 2083
 2084
 2085
 2086
 2087
 2088
 2089
 2090
 2091
 2092
 2093
 2094
 2095
 2096
 2097
 2098
 2099
 2100
 2101
 2102
 2103
 2104
 2105
 2106
 2107
 2108
 2109
 2110
 2111
 2112
 2113
 2114
 2115
 2116
 2117
 2118
 2119
 2120
 2121
 2122
 2123
 2124
 2125
 2126
 2127
 2128
 2129
 2130
 2131
 2132
 2133
 2134
 2135
 2136
 2137
 2138
 2139
 2140
 2141
 2142
 2143
 2144
 2145
 2146
 2147
 2148
 2149
 2150
 2151
 2152
 2153
 2154
 2155
 2156
 2157
 2158
 2159
 2160
 2161
 2162
 2163
 2164
 2165
 2166
 2167
 2168
 2169
 2170
 2171
 2172
 2173
 2174
 2175
 2176
 2177
 2178
 2179
 2180
 2181
 2182
 2183
 2184
 2185
 2186
 2187
 2188
 2189
 2190
 2191
 2192
 2193
 2194
 2195
 2196
 2197
 2198
 2199
 2200
 2201
 2202
 2203
 2204
 2205
 2206
 2207
 2208
 2209
 2210
 2211
 2212
 2213
 2214
 2215
 2216
 2217
 2218
 2219
 2220
 2221
 2222
 2223
 2224
 2225
 2226
 2227
 2228
 2229
 2230
 2231
 2232
 2233
 2234
 2235
 2236
 2237
 2238
 2239
 2240
 2241
 2242
 2243
 2244
 2245
 2246
 2247
 2248
 2249
 2250
 2251
 2252
 2253
 2254
 2255
 2256
 2257
 2258
 2259
 2260
 2261
 2262
 2263
 2264
 2265
 2266
 2267
 2268
 2269
 2270
 2271
 2272
 2273
 2274
 2275
 2276
 2277
 2278
 2279
 2280
 2281
 2282
 2283
 2284
 2285
 2286
 2287
 2288
 2289
 2290
 2291
 2292
 2293
 2294
 2295
 2296
 2297
 2298
 2299
 2300
 2301
 2302
 2303
 2304
 2305
 2306
 2307
 2308
 2309
 2310
 2311
 2312
 2313
 2314
 2315
 2316
 2317
 2318
 2319
 2320
 2321
 2322
 2323
 2324
 2325
 2326
 2327
 2328
 2329
 2330
 2331
 2332
 2333
 2334
 2335
 2336
 2337
 2338
 2339
 2340
 2341
 2342
 2343
 2344
 2345
 2346
 2347
 2348
 2349
 2350
 2351
 2352
 2353
 2354
 2355
 2356
 2357
 2358
 2359
 2360
 2361
 2362
 2363
 2364
 2365
 2366
 2367
 2368
 2369
 2370
 2371
 2372
 2373
 2374
 2375
 2376
 2377
 2378
 2379
 2380
 2381
 2382
 2383
 2384
 2385
 2386
 2387
 2388
 2389
 2390
 2391
 2392
 2393
 2394
 2395
 2396
 2397
 2398
 2399
 2400
 2401
 2402
 2403
 2404
 2405
 2406
 2407
 2408
 2409
 2410
 2411
 2412
 2413
 2414
 2415
 2416
 2417
 2418
 2419
 2420
 2421
 2422
 2423
 2424
 2425
 2426
 2427
 2428
 2429
 2430
 2431
 2432
 2433
 2434
 2435
 2436
 2437
 2438
 2439
 2440
 2441
 2442
 2443
 2444
 2445
 2446
 2447
 2448
 2449
 2450
 2451
 2452
 2453
 2454
 2455
 2456
 2457
 2458
 2459
 2460
 2461
 2462
 2463
 2464
 2465
 2466
 2467
 2468
 2469
 2470
 2471
 2472
 2473
 2474
 2475
 2476
 2477
 2478
 2479
 2480
 2481
 2482
 2483
 2484
 2485
 2486
 2487
 2488
 2489
 2490
 2491
 2492
 2493
 2494
 2495
 2496
 2497
 2498
 2499
 2500
 2501
 2502
 2503
 2504
 2505
 2506
 2507
 2508
 2509
 2510
 2511
 2512
 2513
 2514
 2515
 2516
 2517
 2518
 2519
 2520
 2521
 2522
 2523
 2524
 2525
 2526
 2527
 2528
 2529
 2530
 2531
 2532
 2533
 2534
 2535
 2536
 2537
 2538
 2539
 2540
 2541
 2542
 2543
 2544
 2545
 2546
 2547
 2548
 2549
 2550
 2551
 2552
 2553
 2554
 2555
 2556
 2557
 2558
 2559
 2560
 2561
 2562
 2563
 2564
 2565
 2566
 2567
 2568
 2569
 2570
 2571
 2572
 2573
 2574
 2575
 2576
 2577
 2578
 2579
 2580
 2581
 2582
 2583
 2584
 2585
 2586
 2587
 2588
 2589
 2590
 2591
 2592
 2593
 2594
 2595
 2596
 2597
 2598
 2599
 2600
 2601
 2602
 2603
 2604
 2605
 2606
 2607
 2608
 2609
 2610
 2611
 2612
 2613
 2614
 2615
 2616
 2617
 2618
 2619
 2620
 2621
 2622
 2623
 2624
 2625
 2626
 2627
 2628
 2629
 2630
 2631
 2632
 2633
 2634
 2635
 2636
 2637
 2638
 2639
 2640
 2641
 2642
 2643
 2644
 2645
 2646
 2647
 2648
 2649
 2650
 2651
 2652
 2653
 2654
 2655
 2656
 2657
 2658
 2659
 2660
 2661
 2662
 2663
 2664
 2665
 2666
 2667
 2668
 2669
 2670
 2671
 2672
 2673
 2674
 2675
 2676
 2677
 2678
 2679
 2680
 2681
 2682
 2683
 2684
 2685
 2686
 2687
 2688
 2689
 2690
 2691
 2692
 2693
 2694
 2695
 2696
 2697
 2698
 2699
 2700
 2701
 2702
 2703
 2704
 2705
 2706
 2707
 2708
 2709
 2710
 2711
 2712
 2713
 2714
 2715
 2716
 2717
 2718
 2719
 2720
 2721
 2722
 2723
 2724
 2725
 2726
 2727
 2728
 2729
 2730
 2731
 2732
 2733
 2734
 2735
 2736
 2737
 2738
 2739
 2740
 2741
 2742
 2743
 2744
 2745
 2746
 2747
 2748
 2749
 2750
 2751
 2752
 2753
 2754
 2755
 2756
 2757
 2758
 2759
 2760
 2761
 2762
 2763
 2764
 2765
 2766
 2767
 2768
 2769
 2770
 2771
 2772
 2773
 2774
 2775
 2776
 2777
 2778
 2779
 2780
 2781
 2782
 2783
 2784
 2785
 2786
 2787
 2788
 2789
 2790
 2791
 2792
 2793
 2794
 2795
 2796
 2797
 2798
 2799
 2800
 2801
 2802
 2803
 2804
 2805
 2806
 2807
 2808
 2809
 2810
 2811
 2812
 2813
 2814
 2815
 2816
 2817
 2818
 2819
 2820
 2821
 2822
 2823
 2824
 2825
 2826
 2827
 2828
 2829
 2830
 2831
 2832
 2833
 2834
 2835
 2836
 2837
 2838
 2839
 2840
 2841
 2842
 2843
 2844
 2845
 2846
 2847
 2848
 2849
 2850
 2851
 2852
 2853
 2854
 2855
 2856
 2857
 2858
 2859
 2860
 2861
 2862
 2863
 2864
 2865
 2866
 2867
 2868
 2869
 2870
 2871
 2872
 2873
 2874
 2875
 2876
 2877
 2878
 2879
 2880
 2881
 2882
 2883
 2884
 2885
 2886
 2887
 2888
 2889
 2890
 2891
 2892
 2893
 2894
 2895
 2896
 2897
 2898
 2899
 2900
 2901
 2902
 2903
 2904
 2905
 2906
 2907
 2908
 2909
 2910
 2911
 2912
 2913
 2914
 2915
 2916
 2917
 2918
 2919
 2920
 2921
 2922
 2923
 2924
 2925
 2926
 2927
 2928
 2929
 2930
 2931
 2932
 2933
 2934
 2935
 2936
 2937
 2938
 2939
 2940
 2941
 2942
 2943
 2944
 2945
 2946
 2947
 2948
 2949
 2950
 2951
 2952
 2953
 2954
 2955
 2956
 2957
 2958
 2959
 2960
 2961
 2962
 2963
 2964
 2965
 2966
 2967
 2968
 2969
 2970
 2971
 2972
 2973
 2974
 2975
 2976
 2977
 2978
 2979
 2980
 2981
 2982
 2983
 2984
 2985
 2986
 2987
 2988
 2989
 2990
 2991
 2992
 2993
 2994
 2995
 2996
 2997
 2998
 2999
 3000
 3001
 3002
 3003
 3004
 3005
 3006
 3007
 3008
 3009
 3010
 3011
 3012
 3013
 3014
 3015
 3016
 3017
 3018
 3019
 3020
 3021
 3022
 3023
 3024
 3025
 3026
 3027
 3028
 3029
 3030
 3031
 3032
 3033
 3034
 3035
 3036
 3037
 3038
 3039
 3040
 3041
 3042
 3043
 3044
 3045
 3046
 3047
 3048
 3049
 3050
 3051
 3052
 3053
 3054
 3055
 3056
 3057
 3058
 3059
 3060
 3061
 3062
 3063
 3064
 3065
 3066
 3067
 3068
 3069
 3070
 3071
 3072
 3073
 3074
 3075
 3076
 3077
 3078
 3079
 3080
 3081
 3082
 3083
 3084
 3085
 3086
 3087
 3088
 3089
 3090
 3091
 3092
 3093
 3094
 3095
 3096
 3097
 3098
 3099
 3100
 3101
 3102
 3103
 3104
 3105
 3106
 3107
 3108
 3109
 3110
 3111
 3112
 3113
 3114
 3115
 3116
 3117
 3118
 3119
 3120
 3121
 3122
 3123
 3124
 3125
 3126
 3127
 3128
 3129
 3130
 3131
 3132
 3133
 3134
 3135
 3136
 3137
 3138
 3139
 3140
 3141
 3142
 3143
 3144
 3145
 3146
 3147
 3148
 3149
 3150
 3151
 3152
 3153
 3154
 3155
 3156
 3157
 3158
 3159
 3160
 3161
 3162
 3163
 3164
 3165
 3166
 3167
 3168
 3169
 3170
 3171
 3172
 3173
 3174
 3175
 3176
 3177
 3178
 3179
 3180
 3181
 3182
 3183
 3184
 3185
 3186
 3187
 3188
 3189
 3190
 3191
 3192
 3193
 3194
 3195
 3196
 3197
 3198
 3199
 3200
 3201
 3202
 3203
 3204
 3205
 3206
 3207
 3208
 3209
 3210
 3211
 3212
 3213
 3214
 3215
 3216
 3217
 3218
 3219
 3220
 3221
 3222
 3223
 3224
 3225
 3226
 3227
 3228
 3229
 3230
 3231
 3232
 3233
 3234
 3235
 3236
 3237
 3238
 3239
 3240
 3241
 3242
 3243
 3244
 3245
 3246
 3247
 3248
 3249
 3250
 3251
 3252
 3253
 3254
 3255
 3256
 3257
 3258
 3259
 3260
 3261
 3262
 3263
 3264
 3265
 3266
 3267
 3268
 3269
 3270
 3271
 3272
 3273
 3274
 3275
 3276
 3277
 3278
 3279
 3280
 3281
 3282
 3283
 3284
 3285
 3286
 3287
 3288
 3289
 3290
 3291
 3292
 3293
 3294
 3295
 3296
 3297
 3298
 3299
 3300
 3301
 3302
 3303
 3304